Pharm Res
DOI 10.1007/s11095-012-0817-2

RESEARCH PAPER

A New Strategy to Rapidly Evaluate Kinetics of Glucuronide Efflux by Breast Cancer Resistance Protein (BCRP/ABCG2)

Baojian Wu • Wen Jiang • Taijun Yin • Song Gao • Ming Hu

Received: 7 April 2012 / Accepted: 20 June 2012

ABSTRACT

Purpose The efflux transporter breast cancer resistance protein (BCRP/ABCG2) plays an important role in excretion of anionic drugs and metabolites including glucuronides in humans.

Methods In this article, our recently published cell model (*i.e.*, HeLa cells over-expressing UGT1A9 (HeLa1A9)) is used to determine the kinetic parameters of BCRP-mediated transport of glucuronides.

Results After incubation of the aglycone with the cells, a steady-state (*i.e.*, zero-order or near zero-order) excretion of its glucuronide is rapidly achieved and then maintained. Kinetic profiling with different (intracellular) glucuronide concentrations and their corresponding excretion rates is enabled by varying the concentration of the aglycone, which allows for the determination of kinetic parameters responsible for BCRP-mediated efflux of glucuronides. This approach was validated theoretically using a cellular pharmacokinetic model incorporating various enzymatic and transporter-mediated kinetic processes. It was also validated experimentally in that kinetic parameters of efflux of glucuronides of 6-hydroxyflavone and 4-methylumberiferone in the HeLa1A9 cell model were shown to be consistent with those derived with BCRP-overexpressing membrane vesicles.

Conclusion This study provides a new strategy for rapidly evaluating the kinetics of glucuronide efflux by BCRP.

KEY WORDS BCRP · efflux · glucuronidation · glucuronide · UGT1A9

B. Wu · W. Jiang · T. Yin · S. Gao · M. Hu (✉)
Dept. of Pharmacological & Pharmaceutical Sciences
College of Pharmacy, University of Houston
1441 Moursund Street
Houston, Texas 77030, USA
e-mail: mhu@uh.edu

Published online: 03 July 2012

ABBREVIATIONS

4MU	4-methylumbelliferone
4MU-G	4-methylumbelliferone-glucuronide
6HF	6-hydroxyflavone
6HF-G	6-hydroxyflavone glucuronide
BCRP	breast cancer resistance protein
P-gp	P-glycoprotein
UGTs	UDP-glucuronosyltransferases
UPLC	ultra performance liquid chromatography

INTRODUCTION

The human breast cancer resistance protein (BCRP/ABCG2) is a member of the G subfamily of the large ATP-binding cassette (ABC) transporter superfamily. It is initially known as an efflux pump which renders cancer cells resistant to multiple chemotherapeutic agents such as methotrexate, mitoxantrone, topotecan, SN-38, imatinib and gefitinib (1). In contrast to P-glycoprotein (P-gp) that possesses 12 transmembrane helices (TMs), BCRP is a half transporter with only six TMs. Therefore, two BCRP monomers in a dimeric form are required for transporter functionality (1). In addition, the domain arrangement of BCRP is different from that of P-gp, following a unique "NBD-linker-TMD" pattern (*i.e.*, the nucleotide binding domain (NBD) is located at the N-terminus of the polypeptide chain followed by a linker region and transmembrane domain (TMD)) (2). Nevertheless, the overall experimentally determined topology structure of BCRP is similar to that of mouse P-gp, whose X-ray structure is known (3).

The list of BCRP substrates has been rapidly expanding since its discovery. Aside from chemotherapeutic agents, BCRP substrates include a variety of non-chemotherapy drugs (*e.g.*, glyburide and nitrofurantoin) and chemicals (*e.g.*, hoechst33342) (2). Of note is that most of the BCRP

substrates are structurally unrelated. At present, what determines the substrate specificity of BCRP remains elusive. There is only one structure-activity relationship study for BCRP substrates (*i.e.*, SN-38 and its analogs). This study suggests that camptothecin analogues with high polarity are good substrates for BCRP (4). BCRP is located on the apical membrane of the epithelium of the small intestine and colon, and in the liver canalicular membrane, and its important role in drug/metabolites disposition is now widely recognized. For example, BCRP appears to (negatively) regulate the uptake (availability) of orally administered drugs (*e.g.*, sulfasalazine (5) and irinotecan (6)), and to limit the penetration of topotecan into the central nervous system (7). In recent years, numerous studies have shown that BCRP is involved in intestinal and/or biliary excretion of glucuronides of a diverse group of compounds including harmol (8), acetaminophen (9,10) and dietary flavonoids (11).

Glucuronidation is a significant metabolic pathway that facilitates efficient elimination and detoxification of numerous endo- (*e.g.*, bilirubin and estradiol) and xenobiotics (*e.g.*, SN-38 and indinavir) (12). The involvement of efflux transporters such as BCRP in cellular glucuronide production is necessitated by the fact that glucuronide is too polar to passively diffuse out of cells. Therefore, in addition to UDP-glucuronosyltransferases (UGTs) that catalyze glucuronidation reaction (*i.e.*, glucuronide formation), efflux transporter is another element that enables glucuronide clearance. Impaired BCRP activity could result in reduced (intestinal/hepatic) glucuronide clearance and elevated glucuronide accumulation in systemic circulation (9,11). Moreover, modulation of glucuronide excretion may have important implications with respect to pharmacological and/or adverse effects (8). For example, the side effect diarrhea (a gastrointestinal toxicity) was ameliorated by decreasing the intestinal excretion of SN-38-glucuronide (13).

The BCRP-glucuronide interaction complicates the efforts to predict glucuronidation, and gives rise to the "UGT-BCRP interplay" phenomenon (14,15). Understanding the transport kinetics is of important value in predicting the contribution of BCRP to drug/glucuronide disposition *in vivo*, and/or in determining the rate-limiting step (metabolism *vs.* excretion) of cellular glucuronide production. The transport kinetic parameters (*i.e.*, K_m, V_{max} and CL_{int}= V_{max}/K_m) of efflux transporters are often obtained by the transport assay using plasma membrane (inside-out) vesicles that contains a large amount of the efflux transporter (16). However, the requirement to use purified BCRP substrate for experimentation limits the use of this assay in evaluation of BCRP-mediated glucuronide efflux, usually because of lack of commercial availability of the glucuronides. In this study, we utilize a recently developed engineered cell (*i.e.*, HeLa cells over-expressing UGT1A9, or HeLa1A9 cells) to kinetically determine BCRP-mediated transport of glucuronides (17). One major advantage of our method is that it avoids the use of purified glucuronide. Validation of this method was performed theoretically (*i.e.*, pharmacokinetic modeling and simulation) and experimentally (*i.e.*, the transport kinetic results derived from HeLa1A9 cells were correlated to those from BCRP membrane vesicles).

MATERIALS AND METHODS

Materials

Human BCRP (Arg482) membrane vesicles and expressed UGT1A9 (Supersomes™) were purchased from BD Biosciences (Woburn, MA). 4-Methylumbelliferone (4MU), 4-methylumbelliferone-glucuronide (4MU-G), Leukotriene C4 (LTC4), Ko143, uridine diphosphoglucuronic acid (UDPGA), alamethicin, D-saccharic-1,4-lactone monohydrate, magnesium chloride, and Hanks' balanced salt solution (HBSS, powder form) were purchased from Sigma-Aldrich (St Louis, MO). Ammonium acetate and Tris-HCl were purchased from J.T. Baker (Phillipsburg, NT). 6-Hydroxylfavone (6HF) was purchased from Indofine Chemicals (Somerville, NJ). 6-Hydroxyflavone glucuronide (6HF-G)) was synthesized as described previously (18,19). GF/F glass fiber filters were obtained from Whatman (Piscataway, NJ). All other materials (typically analytical grade or better) were used as received.

Cell Culture

UGT1A9 transfected HeLa cells (referred to as HeLa1A9 cells in this paper) were seeded into Transwells™ at a density of 100,000 cells/well, and were grown using Dulbecco's modified Eagle's medium supplemented with 10% fetal bovine serum. Cells from 2 to 3 days past seeding were used for the experiments. Detailed molecular characterizations on HeLa1A9 cells were performed previously and published (17). Direct determination of HeLa1A9 cell volume is not reported. Nevertheless, for Caco-2 cells, the cell volume was estimated to be 3.66 μl/mg protein (20) by geometrical estimation, and 4.05 μl/mg protein (21) by the cellular accumulation study of sulfanilamide. By analogy, in this study, the HeLa1A9 cell volume was assigned as the average of those two determinations, or 3.86 μl/mg protein (22,23). Based on 3.86 μl/mg protein and 0.99 mg protein/Transwell™, the cell volume for the HeLa1A9 cells grown on a Transwell™ (surface area 4.2 cm^2) is estimated to be 3.82 μl.

Preparation of HeLa Cell Lysate

Membranes of HeLa1A9 cells (from 75 ml flask) cultured for 3 days were disrupted in pH 7.4 HBSS buffer, by sonication

for 15 min in an ice-cold water bath. The protein content of the lysate was determined by the Bio-Rad protein assay kit (Bio-Rad, Hercules, CA), using bovine serum albumin as the standard.

Protein Binding of 6HF, 4MU and Their Glucuronides with HeLa Lysate

The extent of binding of parent compounds and glucuronides (1.6–50 μM) to HeLa1A9 cell lysate was investigated, as described previously (23). The solute was incubated with cell lysate (final lysate protein concentration 0.54 mg/ml) at 37°C for 15 min, and the mixture was rapidly filtered through a filter membrane (3000 mol. wt. cut-off; Millipore Corporation, Billerica, MA) by centrifugation at 15,000 g for 15 min. The control experiment was carried out with the compound present in HBSS buffer, pH 7.4. The filtrate was assayed for protein by Bio-Rad protein assay kit to check for leakiness. Protein binding was calculated according to $\%\text{unbound}=C_u/C\times 100\%$, where C_u is the concentration of the compound in the ultrafiltrate, and C is the concentration of the compound obtained from the filtrate in the control experiment. The samples were analyzed by UPLC.

Glucuronide Excretion Experiments in the HeLa1A9 Cell Model

All culture wells were washed three times with 37°C HBSS (pH 7.4) prior to experimentation. HeLa1A9 cells were incubated in HBSS (2 ml) containing different concentrations of the parent compound (aglycone). The concentrations of the parent compound and the glucuronide in incubation medium were measured by UPLC. Inhibitors, when used, were co-incubated with the aglycone. At each specified time points (*i.e.*, 30, 60, 90, and 120 min, unless otherwise specified), 200 μl samples were taken and then replaced with the same volume of dosing solution (containing the parent compound). After the last time point, the medium was rapidly removed by suction and the cells were washed at least twice with ice-cold HBSS. Intracellular measurements of parent drugs and metabolites were obtained by solubilizing each cell culture well with 500 μl of ice-cold MeOH:H_2O (7:3, v/v) and sonicating the mixture (in an ice-cold ultrasonic bath) for 15 min. The homogenate was centrifuged for 15 min at 15,000 g, and the resulting supernatant was analyzed by UPLC. Glucuronide excretion rate was determined from the excretion rate *vs.* time profile using linear regression (rate equals to the slope).

Glucuronidation Assay

As described previously (24–26), the aglycones (6HF and 4MU) were incubated with expressed UGT1A9 or HeLa1A9 cell lysate. All experiments were performed in triplicates. The incubation medium consisted of 50 mM potassium phosphate buffer (pH=7.4) with 0.88 mM $MgCl_2$, 4.4 mM saccharolactone, 22 μg/ml alamethicin, and 3.5 mM UDPGA (add last). The reaction was terminated by the addition of 50 μl of 94% acetonitrile/6% glacial acetic acid, followed by centrifugation at 15,000 rpm for 15 min. The resultant supernatant was directly subjected to UPLC analysis. Glucuronide(s) formation was verified to be linear with respect to incubation time (30–180 min) and protein concentration (13–53 μg/ml). Glucuronidation rates were calculated as nmol glucuronide(s) formed per reaction time per protein amount (or nmol/min/mg protein).

Pharmacokinetictic Modeling and Simulation

A two-compartment model, consisting of the (incubation) medium and the cell compartments, was used to describe the transport and glucuronidation in HeLa1A9 cells (Fig. 1a, b). The mass balance equations were shown (eqs. 1–4). Transport of the aglycone (A) across the cell membrane occurs with the rate constants K_{in} and K_{out}, representing the summation of passive diffusion and active transport. Glucuronide (G) formation and excretion follow Michaelis–Menten (saturable) kinetics described by V_{max} and K_m, and J_{max} and K'_m, respectively. f_a and f_g denote the unbound fractions of aglycone and conjugate in the cell compartment, respectively. The model assumes (1) glucuronidation is the only metabolic pathway; (2) there is no conversion of glucuronide back to the aglycone (deglucurondation); (3) transport of aglycone across the membrane is a non-saturable (linear) process. All simulations were performed using MATLAB® (The Mathsworks Inc, Natick, MA). The glucuronide excretion data at the 30, 60, 90, or 120 min were used to calculate the excretion rates. In all simulations, the protein binding of glucuronide was assumed to be unity (f_g=1).

$$\frac{dA_m}{dt} = -K_{in}A_m + K_{out}f_aA_c \tag{1}$$

$$\frac{dA_c}{dt} = K_{in}A_m - K_{out}f_aA_c - \frac{f_aA_cV_{max}}{f_aA_c + V_cK_m} \tag{2}$$

$$\frac{dG_m}{dt} = \frac{f_gG_cJ_{max}}{f_gG_c + V_cK'_m} \tag{3}$$

$$\frac{dG_c}{dt} = \frac{f_aA_cV_{max}}{f_aA_c + V_cK_m} - \frac{f_gG_cJ_{max}}{f_gG_c + V_cK'_m} \tag{4}$$

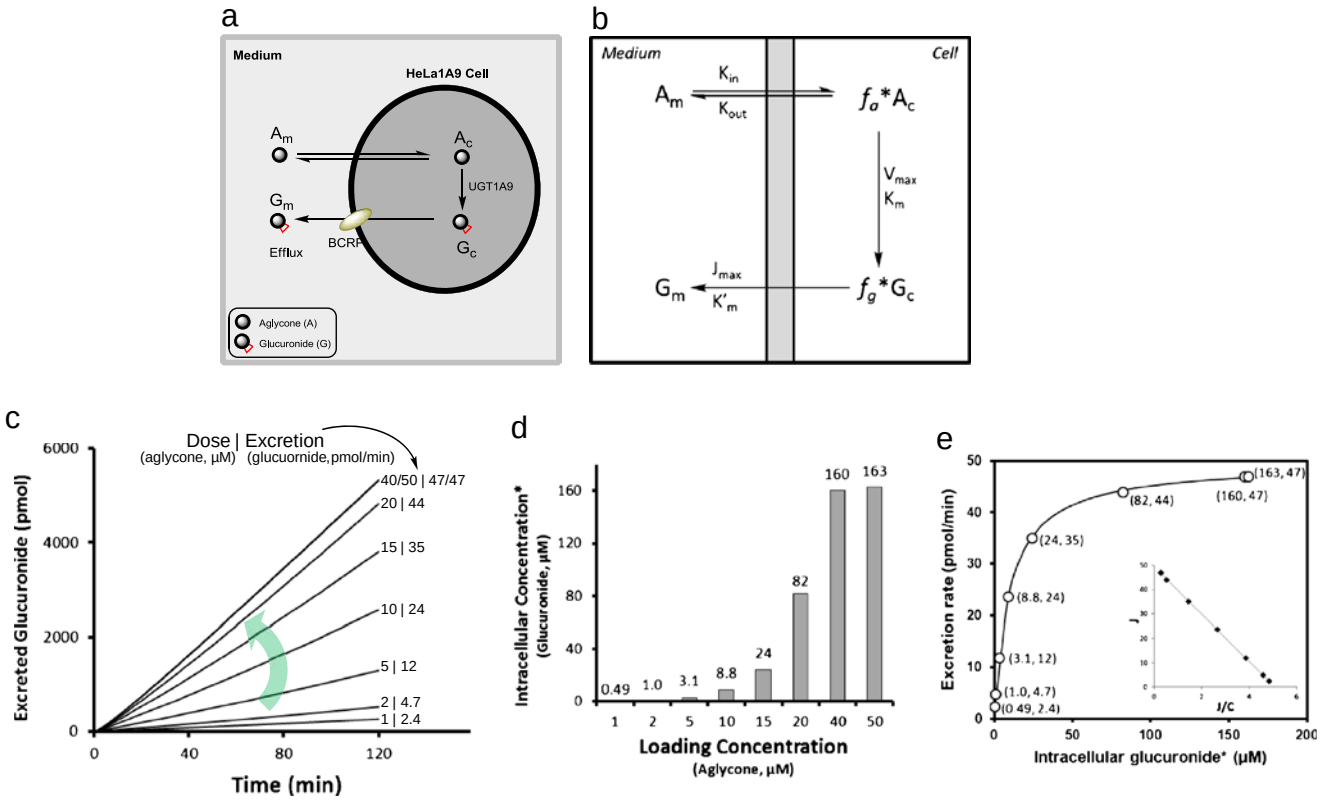

Fig. 1 Use of a pharmacokinetic model to illustrate kinetic profiling of BCRP with glucuronide in this study. (**a**) Schematic presentation of the steady-state glucuronide formation (by UGT1A9) and excretion (by BCRP) in HeLa1A9 cell model. (**b**) Schematic presentation of a two-compartment model that describes the glucuronidation in HeLa1A9 cells. (**c**, **d**) Simulated excretion profiles and intracellular concentration for glucuronide based on the pharmacokinetic model. (**e**) Plot of the excretion rates *vs.* intracellular concentrations, the inset shows the Eadie-Hofstee plot. (**c**-**e**) Simulations were performed using the following parameter values, V_{cell}=4 μl, V_{medium}=2000 μl, K_{in}=K_{out}=0.001 min^{-1}, K_m=1 μM, K'_m=10 μM, V_{max}=J_{max}=50 pmol/min.

Kinetics Analysis

Kinetic parameters (V_{max} and K_m for glucuronide formation; J_{max} and K'_m for glucuronide excretion) were estimated by fitting Michaelis-Menten equation to the data by nonlinear least-squares regression using a weighting of 1/y. Data analysis was performed by GraphPad Prism V5 for Windows (GraphPad Software, San Diego, CA). The goodness of fit was evaluated on the basis of R^2 values, RSS (residual sum of squares), RMS (root mean square) and residual plots.

Vesicular Transport Studies for BCRP

Vesicular transport studies were performed with rapid filtration techniques as described previously (27–29). In brief, membrane fractions containing inside out efflux transporters were incubated in the presence or absence of 5 mM ATP in a buffer containing 10 mM $MgCl_2$ and 10 mM Tris/HCl (pH 7.4). The transport was stopped by addition of 1 ml of cold transport buffer to the membrane suspensions and then rapidly filtered through class F glass fiber filters (pore size, 0.45 μm). Filters were washed with 2× 5 ml of ice-cold wash buffer, cut and transferred to a 1.5-ml Eppendorf tube containing 400 μl of 50% methanol, followed by sonicating for 15 min. After centrifugation at 15,000 rpm for 15 min, the supernatant was subjected into UPLC quantitative analysis. ATP-dependent transport was calculated by subtracting the values obtained in the presence of AMP from those in the presence of ATP.

UPLC Analysis

The Waters ACQUITY™ UPLC (Ultra performance liquid chromatography) system was used to analyze the parent compounds and their respective glucuronides. The UPLC condition was described in our earlier publications (24–26).

Statistical Analysis

One-way ANOVA with or without Tukey-Kramer multiple comparison (post hoc) tests was used to evaluate statistical

differences. Differences were considered significant when p values were less than 0.05 ($p<0.05$).

RESULTS AND DISCUSSION

Theoretical Validation of HeLa1A9 Cells to Determine Kinetic Parameters for BCRP with Glucuronides

Glucuronide formation and excretion in HeLa1A9 cells were simulated based on a two-compartment pharmacokinetic model (Fig. 1a, b) and varied model parameters (Table I). Interestingly, a steady-state (*i.e.*, zero-order or near zero-order) excretion for glucuronide is observed (Fig. 1c). When the aglycone dose (for incubation) is increased, both excretion rate and the intracellular concentration (for glucuronide) also increased (Fig. 1c, d). The kinetic parameters were derived by plotting the excretion rates *vs.* the glucuronide concentrations (Fig. 1e). Using this approach, we have estimated the kinetic constants (K'_m and J_{max}) based on simulation data and compared them with the assigned (true) values (Table I). The estimates are close or identical to the true values, suggesting that our model may be used for determining the kinetics of BCRP-mediated glucuronide transport.

Experimental Validation of HeLa1A9 Cells to Determine Kinetic Parameters for BCRP with Glucuronides

In this paper, we mainly used 6-hydroxyflavone (6HF) and 4-methylumbelliferone (4MU) and their glucuronides (see Fig. 2a for chemical structures) to validate the potential values of HeLa1A9 cell model in determination of the kinetic parameters for BCRP-mediated efflux of glucuronides. The two compounds were selected because of their distinct physicochemical properties such as logP and protein binding, as well as the glucuronidation susceptibility (see below).

Binding of 6HF to HeLa1A9 cell lysate protein was extensive, whereas binding of 4MU was modest (Fig. 2b, c). The unbound fractions of 6HF and 4MU (1.6–50 μM) were <0.02% and 40%–57%, respectively. By contrast, as expected, binding of the polar glucuronides to HeLa1A9

Table I Correlations Between the Assigned (True) and Estimated Values* (for K'_m and J_{max}) at Various Model Parameters

Assigned K'_m μM	Assigned J_{max} pmol/min	f_a	K_{in} Min^{-1}	K_{out} Min^{-1}	K_m μM	V_{max} pmol/min	Estimated K'_m * μM	Estimated J_{max} * pmol/min
1	50	1	0.0005	0.0005	1	50	1.00	50.1
1	50	1	0.001	0.001	1	50	0.98	49.7
1	50	1	0.001	0.01	1	50	0.97	49.7
1	50	1	0.001	0.1	1	50	0.98	49.9
1	50	1	0.005	0.005	1	50	0.97	50.5
1	50	0.8	0.001	0.001	1	50	0.98	49.7
1	50	0.5	0.001	0.001	1	50	0.98	49.7
1	50	0.1	0.001	0.001	1	50	0.98	49.6
1	50	1	0.001	0.001	10	50	0.98	49.7
1	50	1	0.001	0.001	100	50	1.00	49.5
1	50	1	0.001	0.001	1	80	0.98	49.8
1	50	1	0.001	0.001	1	100	0.98	49.8
5	50	1	0.001	0.001	1	50	4.88	49.6
10	50	1	0.001	0.001	1	50	9.75	49.6
20	50	1	0.001	0.001	1	50	19.6	49.4
50	50	1	0.001	0.001	1	50	48.9	49.3
100	50	1	0.001	0.001	1	50	98.9	49.2
1	5	1	0.001	0.001	1	100	0.96	4.93
1	10	1	0.001	0.001	1	100	0.98	9.99
1	20	1	0.001	0.001	1	100	0.98	20.0
1	100	1	0.001	0.001	1	100	1.00	98.8

*Based on simulation data using the two-compartment model (Fig. 1b).

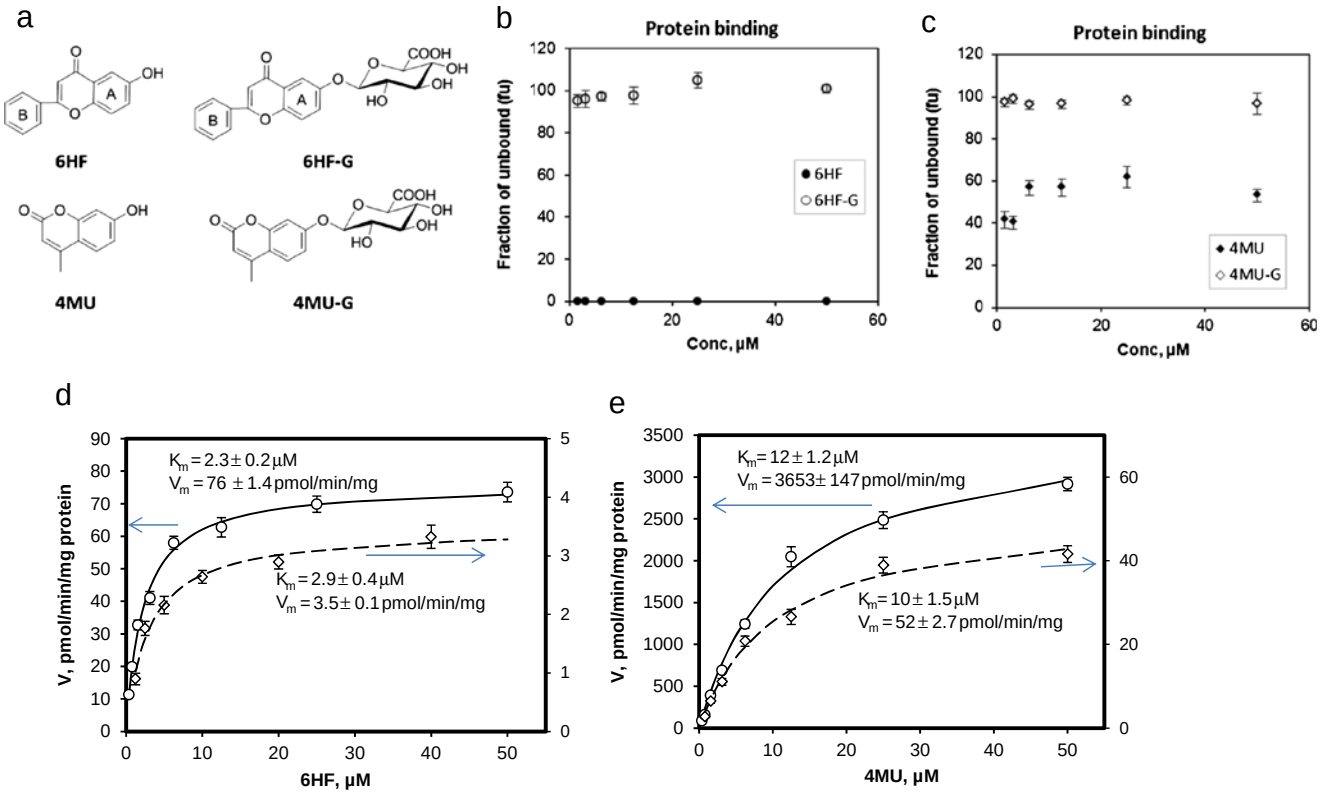

Fig. 2 Protein binding and glucuronidation characterization. (**a**) Chemical structures of 6HF and 4MU and their glucuronides. (**b**) Protein binding of 6HF and its glucuronide (1.6–50 μM) to HeLa1A9 cell lysate. (**c**) Protein binding of 4MU and its glucuronide (1.6–50 μM) to HeLa1A9 cell lysate. (**d**) Kinetic profiles of glucuronidation derived from incubation of 6HF with HeLa1A9 cell lysate (*diamonds*) and recombinant UGT1A9 (*circles*). (**e**) Kinetic profiles of glucuronidation derived from incubation of 4MU with HeLa1A9 cell lysate (*diamonds*) and recombinant UGT1A9 (*circles*).

cell lysate protein was negligible (Fig. 2b, c). The unbound fractions of 6HF-G and 4MU-G (1.6–50 μM) were 95%–104% and 96%–99%, respectively.

UGTs present in HeLa1A9 cell lysate glucuronidated 6HF and 4MU with K_m values similar ($p>0.05$) to those derived using recombinant UGT1A9 (2.9 *vs.* 2.3 μM for 6HF; 10 *vs.* 12 μM for 4MU) (Fig. 2d, e). However, compared to recombinant UGT1A9, HeLa1A9 cell lysate exhibited much smaller V_{max} values (3.5 *vs.* 76 pmol/min/mg for 6HF; 52 *vs.* 3653 pmol/min/mg for 4MU) (Fig. 2d, e), suggesting that HeLa1A9 cell lysate had a much lower UGT1A9 expression. Although 6HF and 4MU were significantly bound to HeLa1A9 cell lysate (Fig. 2b, c), the K_m values were not corrected for protein binding. This is because the nonspecific binding of 6HF and 4MU estimated using the Hallifax-Houston model (30) under the incubation conditions (26.5 μg/ml protein) was less than 5%. Similar to an earlier study (31), the logP values (6HF, 3.12; 4MU, 1.95) used for the protein binding estimation were calculated with the Molinspiration property calculator (http://www.molinspiration.com/services/logp.html).

The key role of BCRP in excretion of glucuronide was determined by inhibition studies. When LTC4 (a specific inhibitor of multidrug resistance proteins (MRPs), 0.1–0.4 μM) was applied, glucuronidation in HeLa1A9 cells was not affected at all, since no changes were observed in the amounts of excreted glucuronide or the intracellular glucuronide or intracellular aglycones (Fig. 3a, c). By contrast, inhibition of BCRP by a specific inhibitor Ko143 (5–20 μM) (32) resulted in significantly reduced glucuronide excretion but elevated accumulation of intracellular glucuronide (Fig. 3b, c). The inhibitory effect on excretion rate was dose-dependent ($p<0.05$), and the extent of decreases were 11%, 16%, and 32% at 5, 10 and 20 μM Ko143, respectively. At the same time, the intracellular concentrations of glucuronide were increased by 2.9-, 4.3-, and 9.8-fold at 5, 10 and 20 μM Ko143, respectively. As a result, the apparent glucuronide clearance (CL_{app}=excretion rate/intracellular level) was decreased by 2.7-, 4.1-, 12.6-fold at 5, 10 and 20 μM Ko143, respectively (Fig. 3d). It was suggested that deglucuronidation (or β-glucuronidase) activity is none or minimal, since total amount of formed glucuronide (*i.e.*, sum of excreted and accumulated glucuronide) was not altered ($p>0.05$) by efflux inhibition. The data consistently indicated that BCRP not MRPs was responsible for the glucuronide excretion in HeLa1A9 cells. The main role of BCRP in excretion of glucuronide in HeLa1A9 cell model was also confirmed by inhibition studies using 4MU (data not shown) and other compounds, as well as

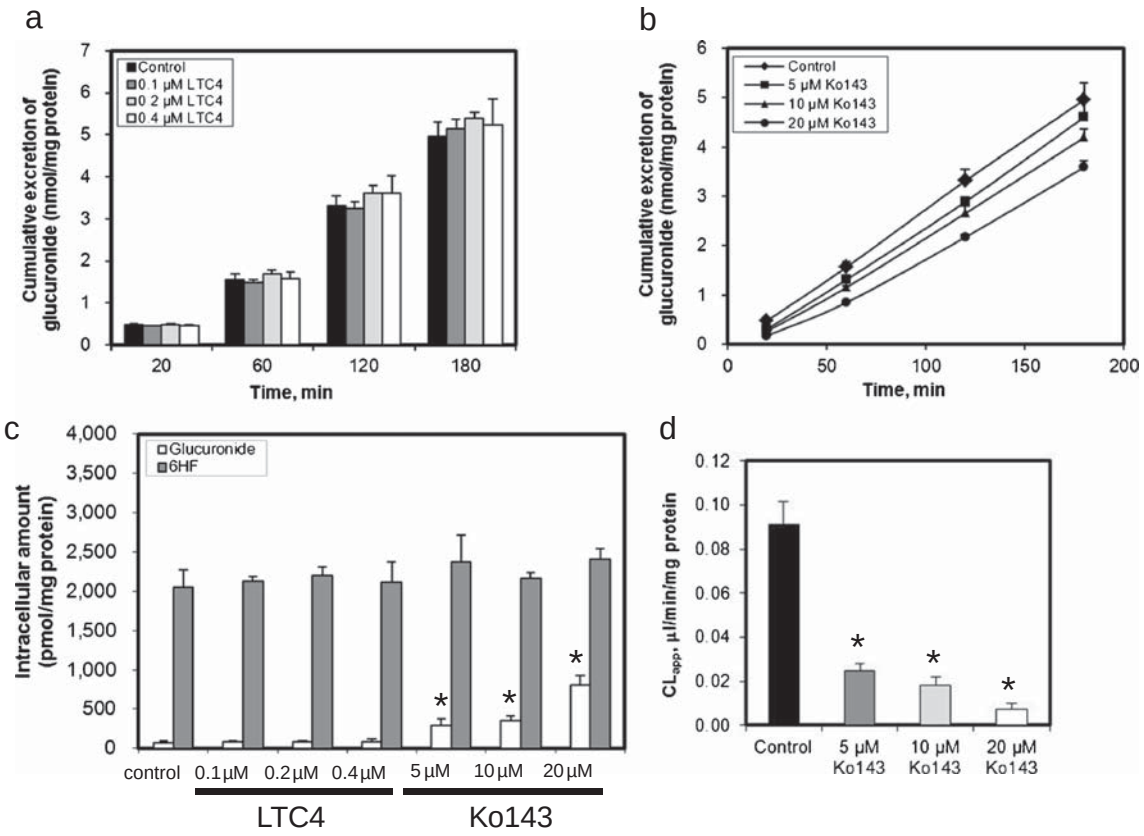

Fig. 3 Inhibition of glucuronidation of 6-hydroxyflavone (6HF) by Leukotriene C4 (LTC4, a specific inhibitor for MRPs) and Ko143 (a specific inhibitor for BCRP) in HeLa1A9 cell model. (**a**) Cumulative excretion of 6-hydroxyflavone glucuronide (6HF-G) in HeLa1A9 cell model after a dose of 10 μM 6HF, showing that the excretion was not affected by the use of LTC4 (0.1–0.4 μM). (**b**) Cumulative excretion of 6HF-G in HeLa1A9 cell model, showing that the excretion was significantly decreased ($p < 0.05$) by Ko143 (5–20 μM). (**c**) The intracellular levels of 6HF and its glucuronide at the end of experiment (3 h). (**d**) Apparent clearance (= excretion rate/intracellular glucuronide) was decreased by Ko143 (5–20 μM). The asterisk (*) indicates statistical differences ($p < 0.05$) between control and treatment groups.

molecular characterization on potential efflux transporters (17). Of note, the expression of MRP2 and MRP3, two potential glucuronide transporters, were not detected (17).

Some aglycones such as flavonoids were reported to be either BCRP inhibitors or substrates (33,34). To rule out the possibility that the aglycone itself might interfere with the glucuronide-BCRP interaction, we confirmed that SN-38 (a BCRP substrate) or biochanin A (a potential inhibitor) (16,33), dosed at 10 μM did not affect the glucuronidation of 6HF (1–50 μM) in HeLa1A9 cell model (data not shown). On the other hand, the excretion of glucuronide in HeLa1A9 cells follows a zero-order kinetic pattern even at high substrate concentrations, which suggests that inhibition of this process is none or minimal. Significant inhibition of glucuronide efflux, if any, would have resulted in an excretion-time profile with a notable time lag as observed in Fig. 3b. Therefore, the impact of tested aglycone itself (≤10 μM) on the excretion of its glucuronide *via* BCRP inhibition should be negligible in HeLa1A9 cells under the current experimental conditions.

The excretion of 6HF-G followed a (near) zero-order kinetic pattern under various 6HF concentrations (0.5–50 μM) (Fig. 4a). By varying the loading concentration, intracellular concentration (at the end of experiment or 120 min) of 6HF-G was altered accordingly (Fig. 4b). Therefore, the integration of the different (intracellular) 6HF-G concentrations with their corresponding excretion rates enabled us to derive the transport kinetic parameters. The obtained K_m value for BCRP-mediated transport of 6HF-G was comparable ($p > 0.05$) to that from BCRP membrane vesicles (15 *vs.* 23 μM, Fig. 4c). However, the V_{max} values differed by 6.6 –fold, probably due to the differences in BCRP expression level. The same approach was applied to determine the kinetic parameters for BCRP-mediated transport of 4MU-G (Fig. 4d–f). The obtained K_m value was very close ($p > 0.05$) to that from BCRP membrane vesicles (24 *vs.* 27 μM, Fig. 4f), whereas V_{max} value was 6.6-fold lower than that determined using BCRP membrane vesicles as observed for 6HF-G.

It is noteworthy that the use of HeLa1A9 cell model to study BCRP-glucuronide interaction is limited to those glucuronides whose precursors (aglycones) are at least fare substrates of UGT1A9. No glucuronide excretion was observed when incubating very poor UGT1A9 substrates such

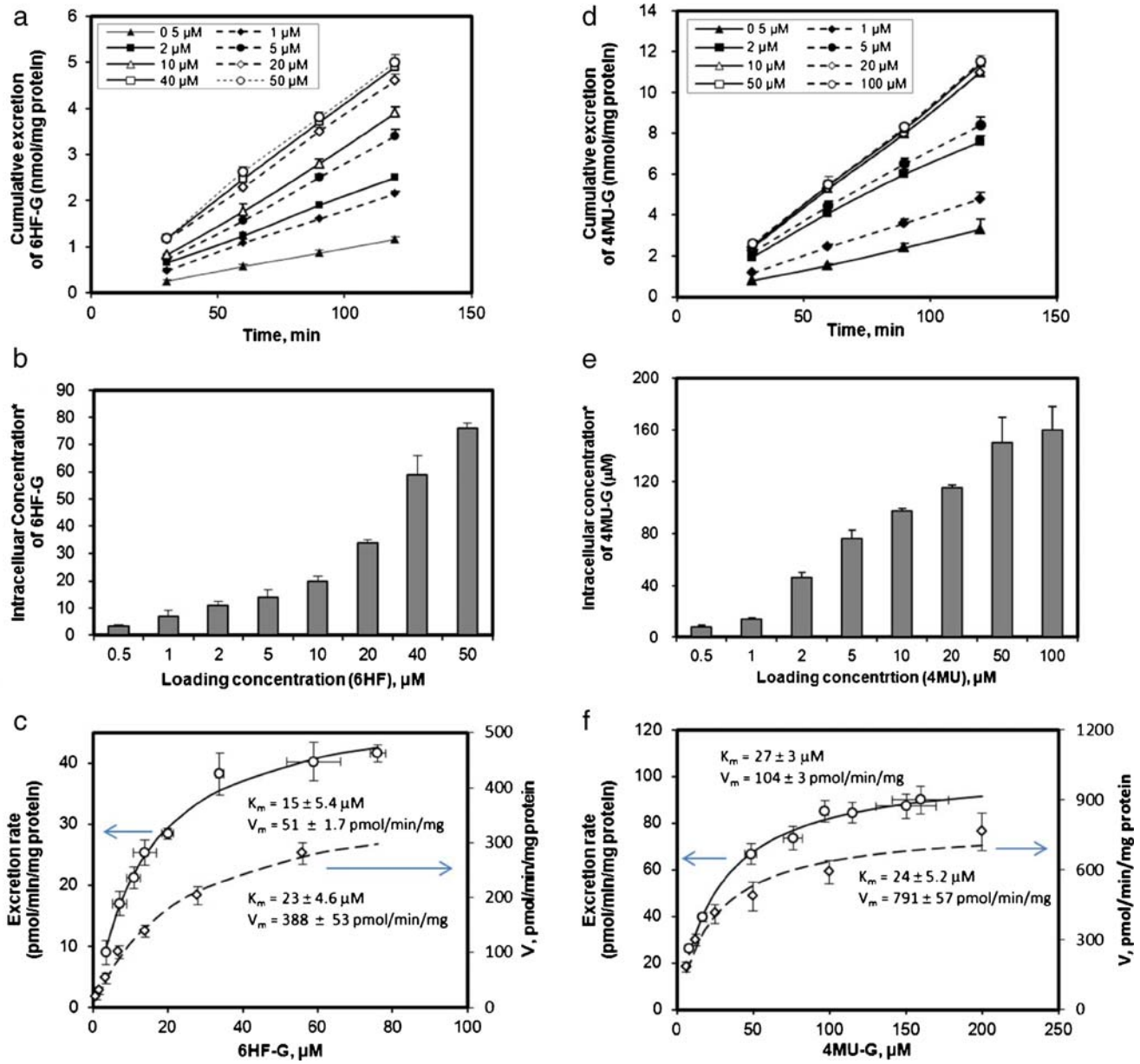

Fig. 4 Transport kinetics of BCRP with glucuronides derived using HeLa1A9 cells. (**a**) Glucuronide excretion-time profile after different 6HF doses (0.5–50 μM), showing loading-dose dependent excretion of glucuronide. (**b**) Intracellular 6HF concentration was altered with the changes in loading concentration. (**c**) Kinetic profiles of BCRP-mediated transport of 6HF-G using the HeLa1A9 cells (*circles*) and BCRP membrane vesicles (*diamonds*). (**d**) Glucuronide excretion-time profile after different 4MU doses (0.5–100 μM), showing loading-dose dependent excretion of glucuronide. (**e**) Intracellular 4MU-G concentration is altered with the changes in loading concentration (4MU). (**f**) Kinetic profiles of BCRP-mediated transport of 4MU-G using the HeLa1A9 cells (*circles*) and BCRP membrane vesicles (*diamonds*).

as estradiol and ezetimibe with HeLa1A9 cells, thus precluding evaluation of BCRP interaction with their glucuronides. In addition, the aglycone should be permeable to gain access to inside of the cells. A logP value of 1.85~6.46 might be necessary based on a screening of 27 structurally diverse aglycones dosed at a concentration of 10 μM (data not shown). Studies are ongoing to derive the activity of BCRP towards structurally diverse glucuronides and to establish the quantitative structure-activity relationships.

CONCLUSION

Understanding of BCRP-glucuronide interaction and the kinetics should facilitate predictions of BCRP-mediated glucuronide clearance *in vivo*. In this paper, we propose a new strategy to determine the kinetic parameters of BCRP-mediated glucuronide efflux using the HeLa1A9 cells. The proposed strategy is based on the measurement of intracellular glucuronide concentrations and the corresponding excretion rates of glucuronides after loading different concentrations of

the parent compounds on the HeLa1A9 cells. The results indicated that the use of new HeLa1A9 cell model represents a viable new strategy to rapidly evaluate the kinetics of interaction between glucuronides and efflux transporters.

ACKNOWLEDGMENTS AND DISCLOSURES

This work was supported by grants from the National Institutes of Health (GM070737) to MH.

REFERENCES

1. Doyle LA, Ross DD. Multidrug resistance mediated by the breast cancer resistance protein BCRP (ABCG2). Oncogene. 2003;22 (47):7340–58.
2. Ni Z, Bikadi Z, Rosenberg MF, Mao Q. Structure and function of the human breast cancer resistance protein (BCRP/ABCG2). Curr Drug Metab. 2010;11(7):603–17.
3. Rosenberg MF, Bikadi Z, Chan J, Liu X, Ni Z, Cai X, Ford RC, Mao Q. The human breast cancer resistance protein (BCRP/ABCG2) shows conformational changes with mitoxantrone. Structure. 2010;18(4):482–93.
4. Yoshikawa M, Ikegami Y, Hayasaka S, Ishii K, Ito A, Sano K, Suzuki T, Togawa T, Yoshida H, Soda H, Oka M, Kohno S, Sawada S, Ishikawa T, Tanabe S. Novel camptothecin analogues that circumvent ABCG2-associated drug resistance in human tumor cells. Int J Cancer. 2004;110(6):921–7.
5. Zaher H, Khan AA, Palandra J, Brayman TG, Yu L, Ware JA. Breast cancer resistance protein (Bcrp/abcg2) is a major determinant of sulfasalazine absorption and elimination in the mouse. Mol Pharm. 2006;3(1):55–61.
6. Stewart CF, Leggas M, Schuetz JD, Panetta JC, Cheshire PJ, Peterson J, Daw N, Jenkins 3rd JJ, Gilbertson R, Germain GS, Harwood FC, Houghton PJ. Gefitinib enhances the antitumor activity and oral bioavailability of irinotecan in mice. Cancer Res. 2004;64(20):7491–9.
7. Zhuang Y, Fraga CH, Hubbard KE, Hagedorn N, Panetta JC, Waters CM, Stewart CF. Topotecan central nervous system penetration is altered by a tyrosine kinase inhibitor. Cancer Res. 2006;66(23):11305–13.
8. Zamek-Gliszczynski MJ, Hoffmaster KA, Nezasa K, Tallman MN, Brouwer KL. Integration of hepatic drug transporters and phase II metabolizing enzymes: mechanisms of hepatic excretion of sulfate, glucuronide, and glutathione metabolites. Eur J Pharm Sci. 2006;27(5):447–86.
9. Zamek-Gliszczynski MJ, Hoffmaster KA, Humphreys JE, Tian X, Nezasa K, Brouwer KL. Differential involvement of Mrp2 (Abcc2) and Bcrp (Abcg2) in biliary excretion of 4-methylumbelliferyl glucuronide and sulfate in the rat. J Pharmacol Exp Ther. 2006;319(1):459–67.
10. Lee JK, Abe K, Bridges AS, Patel NJ, Raub TJ, Pollack GM, Brouwer KL. Sex-dependent disposition of acetaminophen sulfate and glucuronide in the *in situ* perfused mouse liver. Drug Metab Dispos. 2009;37(9):1916–21.
11. Xu H, Kulkarni KH, Singh R, Yang Z, Wang SW, Tam VH, Hu M. Disposition of naringenin via glucuronidation pathway is affected by compensating efflux transporters of hydrophilic glucuronides. Mol Pharm. 2009;6(6):1703–15.
12. Wu B, Kulkarni K, Basu S, Zhang S, Hu M. First-pass metabolism via UDP-glucuronosyltransferase: a barrier to oral bioavailability of phenolics. J Pharm Sci. 2011;100(9):3655–81.
13. Horikawa M, Kato Y, Sugiyama Y. Reduced gastrointestinal toxicity following inhibition of the biliary excretion of irinotecan and its metabolites by probenecid in rats. Pharm Res. 2002;19:1345–53.
14. Jeong EJ, Liu X, Jia X, Chen J, Hu M. Coupling of conjugating enzymes and efflux transporters: impact on bioavailability and drug interactions. Curr Drug Metab. 2005;6(5):455–68.
15. Liu Z, Hu M. Natural polyphenol disposition via coupled metabolic pathways. Expert Opin Drug Metab Toxicol. 2007;3(3):389–406.
16. Nakatomi K, Yoshikawa M, Oka M, Ikegami Y, Hayasaka S, Sano K, Shiozawa K, Kawabata S, Soda H, Ishikawa T, Tanabe S, Kohno S. Transport of 7-ethyl-10-hydroxycamptothecin (SN-38) by breast cancer resistance protein ABCG2 in human lung cancer cells. Biochem Biophys Res Commun. 2001;288(4):827–32.
17. Jiang W, Xu B, Wu B, Yu R, Hu M. UDP-glucuronosyltransferase (UGT) 1A9-overexpressing HeLa cells is an appropriate tool to delineate the kinetic interplay between breast cancer resistance protein (BRCP) and UGT and to rapidly identify the glucuronide substrates of BCRP. Drug Metab Dispos. 2012;40(2):336–45.
18. Joseph TB, Wang SW, Liu X, Kulkarni KH, Wang J, Xu H, Hu M. Disposition of flavonoids via enteric recycling: enzyme stability affects characterization of prunetin glucuronidation across species, organs, and UGT isoforms. Mol Pharm. 2007;4 (6):883–94.
19. Wu B, Xu B, Hu M. Regioselective glucuronidation of flavonols by six human UGT1A isoforms. Pharm Res. 2011;28(8):1905–18.
20. Blais A, Bissonnette P, Berteloot A. Common characteristics for Na + -dependent sugar transport in Caco-2 cells and human fetal colon. J Membr Biol. 1987;99(2):113–25.
21. Yamaguchi H, Yano I, Hashimoto Y, Inui KI. Secretory mechanisms of grepafloxacin and levofloxacin in the human intestinal cell line caco-2. J Pharmacol Exp Ther. 2000;295:360–6.
22. Sun H, Pang KS. Permeability, transport, and metabolism of solutes in Caco-2 cell monolayers: a theoretical study. Drug Metab Dispos. 2008;36(1):102–23.
23. Sun H, Zhang L, Chow EC, Lin G, Zuo Z, Pang KS. A catenary model to study transport and conjugation of baicalein, a bioactive flavonoid, in the Caco-2 cell monolayer: demonstration of substrate inhibition. J Pharmacol Exp Ther. 2008;326(1):117–26.
24. Wu B, Morrow JK, Singh R, Zhang S, Hu M. Three-dimensional quantitative structure-activity relationship studies on UGT1A9-mediated 3-O-glucuronidation of natural flavonols using a pharmacophore-based comparative molecular field analysis model. J Pharmacol Exp Ther. 2011;336(2):403–13.
25. Singh R, Wu B, Tang L, Liu Z, Hu M. Identification of the position of mono-O-glucuronide of flavones and flavonols by analyzing shift in online UV spectrum (lambdamax) generated from an online diode array detector. J Agric Food Chem. 2010;58 (17):9384–95.
26. Singh R, Wu B, Tang L, Hu M. Uridine diposphate glucuronosyltransferases isoform-dependent regiospecificity of glucuronidation of flavonoids. J Agric Food Chem. 2011;59(13): 7452–64.
27. Bodo A, Bakos E, Szeri F, Varadi A, Sarkadi B. Differential modulation of the human liver conjugate transporters MRP2 and MRP3 by bile acids and organic anions. J Biol Chem. 2003; 278:23529–37.
28. Hu Y, Sampson KE, Heyde BR, Mandrell KM, Li N, Zutshi A, Lai Y. Saturation of multidrug-resistant protein 2 (mrp2/abcc2)-mediated hepatobiliary secretion: nonlinear pharmacokinetics of a heterocyclic compound in rats after intravenous bolus administration. Drug Metab Dispos. 2009;37(4):841–6.
29. Pál A, Méhn D, Molnár E, Gedey S, Mészáros P, Nagy T, Glavinas H, Janáky T, von Richter O, Báthori G, Szente L, Krajcsi P. Cholesterol potentiates ABCG2 activity in a heterologous expression

system: improved *in vitro* model to study function of human ABCG2. J Pharmacol Exp Ther. 2007;321(3):1085–94.
30. Hallifax D, Houston JB. Binding of drugs to hepatic microsomes: comment and assessment of current prediction methodology with recommendation for improvement. Drug Metab Dispos. 2006;34 (4):724–6.
31. Zhou J, Tracy TS, Remmel RP. Glucuronidation of dihydrotestosterone and trans-androsterone by recombinant UDP-glucuronosyltransferase (UGT) 1A4: evidence for multiple UGT1A4 aglycone binding sites. Drug Metab Dispos. 2010;38(3):431–40.
32. Pick A, Klinkhammer W, Wiese M. Specific inhibitors of the breast cancer resistance protein (BCRP). ChemMedChem. 2010;5 (9):1498–505.
33. Zhang S, Yang X, Coburn RA, Morris ME. Structure activity relationships and quantitative structure activity relationships for the flavonoid-mediated inhibition of breast cancer resistance protein. Biochem Pharmacol. 2005;70(4):627–39.
34. An G, Gallegos J, Morris ME. The bioflavonoid kaempferol is an Abcg2 substrate and inhibits Abcg2-mediated quercetin efflux. Drug Metab Dispos. 2011;39(3):426–32.